Historical reconstruction of Total Solar Irradiance and forecast of solar magnetic activity for SC-25

V. Penza[1], F. Berrilli[1], L. Bertello[2], M. Cantoresi[1], S. Criscuoli[2]

[1] Department of Physics, University of Rome Tor Vergata, [2] National Solar Observer

Penza et al., 2022, ApJ 937, 84

Penza et al., 2023, Rendiconti Lincei

Abstract

Reconstruction of the Total Solar Irradiance (TSI) over past epochs requires the evaluation of two major temporal components of solar activity: the quasi-cyclical component due to the 11-year sunspot cycle and the long-term component.
We present here an empirical method to separate these components and to estimate the levels of the TSI during the last five centuries, an important information for global or regional climatology studies. We used available historical records of active region area coverage, reproduced by a functional form, and a time series of the Solar Modulation Potential to which we apply the Hilbert-Huang empirical mode decomposition (EMD) algorithm. The main finding of our study is that the estimated TSI values during the Maunder minimum and the present epoch differ by ~ 2.5 W/m^2. By using this approach, we are also able to forecast the area coverage of active regions for solar cycle 25.

Introduction

Solar variability involves all spatial, temporal, and wavelength scales. Its primary driver is the magnetic 11-y cycle. During this cycle, the Sun's magnetic activity increases and weakens. As a result, the area fraction of bright (plages) and dark (sunspots) active regions over the solar surface changes in phase with the magnetic activity.
The total solar irradiance (TSI) varies between minimum and maximum of a cycle of about 0.1%. These changes are not uniform across all wavelengths and Spectral Solar Irradiance (SSI) can show much larger variations.
To reconstruct long term variations of TSI we have to estimate both the variations of plage, sunspot, etc., and the possible contribution of an open magnetic field long-term component. Here we propose an empirical method to reconstruct TSI variations from 1513 CE to present, based on the empirical mode decomposition of the solar modulation potential (ϕ) and on the observed properties of different magnetic cycles. With such an approach we estimate the area coverage of sunspot and faculae for a odd cycle (asa 25th cycle) and forecast the 25th solar cycle.

Datasets

The datasets used in this work are:

- The plage area derived from Ca II K spectroheliogram observations covering the period 1892-2019 (Chatzistergos et al., 2019) and the sunspot area for the period 1874-2019 (Mandal, 2020) were available from the MPS website[(1)] at the data December 2021.
- The values of Φ, from 1000 to 2001 A.D., derived from the analysis of the ^{14}C (Muscheler, 2007), are available on the NOAA website[(2)].
- The TSI data are provided by PMOD composite[(3)] and by TSIS/TIM observations at the LASP datacenter[(4)] .
- The Bremen MgII composite and the CLS Solar Radio Flux at 10.7 cm time series are available at the LASP datacenter[(4)]

(1) http://www2.mps.mpg.de/projects/sun-climate/data.html
(2) https://www.ncdc.noaa.gov/paleo-search
(3) https://www.pmodwrc.ch/en/research-development/solar-physics/tsi-composite
(4) https://lasp.colorado.edu/lisird

Reconstruction and forecast of plage and sunspot

Reconstruction: plage and sunspot areas are obtained using the functional form (Volobuev, 2009):

(1) $$z_k(t) = \left(\frac{t-T0_k}{Ts_k}\right)^2 e^{-\left(\frac{t-T0_k}{Td_k}\right)^2} \quad \text{for} \quad T0_k < t < T0_k + \tau_k$$

$T0_k$ = k-cycle starting time
Ts_k = free parameter related to strenght of k-cycle
Td_k = free parameters related to rising time

We found that Ts_k and Td_k are not independent (Walmeyer effect) and that also Ts_k-spot and Ts_k-plage are correlated:

(2) $$Td_k^{plage} = (0.10 \pm 0.02) Ts_k^{plage} + (3.14 \pm 0.33) \quad yr \qquad Ts_k^{spot} = (4.9 \pm 1.4) Ts_k^{plage} - (13.3 \pm 16.4) \quad yr$$
$$Td_k^{spot} = (0.02 \pm 0.01) Ts_k^{spot} + (3.14 \pm 0.43) \quad yr.$$

Therefore, the single parameter Ts_k^{plage} describes the plage and sunspot area over k-cycle. This parameter shows a linear correlation with the solar modulation potential, integrated over the k-cycle duration $<\Phi_k>$:

(3) $$Ts_k^{plage} = -(0.011 \pm 0.002) < \Phi >_k + (18.5 \pm 1.5) \quad yr$$

We use Eq. (3) in order to obtain the values in the temporal periods when measurements were not available and we obtain the composite of the plage and sunspot coverages are shown in Fig. 1.

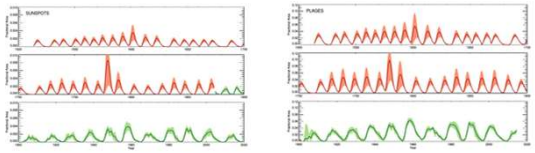

Fig. 1 *Composite of annual values of the fractional solar disk coverage of sunspot (left) and plage (right) as a function of time, obtained by merging the values from the reconstructed time series using Eq.(4) (red solid line) and observed data (green solid line). The light-red region indicates the uncertainty range in the reconstructed time series, while the light-green region shows the 5σ confidence interval of the mean annual value.*

Forecast for 25th Solar Cycle: we identify the following odd–even relationship of the parameters Ts_{2k+1} versus Ts_{2k} for sunspot and plage coverage relations:

(4) $$Ts_e^{plage} = (0.74 \pm 0.08) Ts_o^{plage} + (1.5 \pm 1.1) yr$$
$$Ts_e^{spot} = (0.69 \pm 0.05) Ts_o^{spot} + (11 \pm 3) yr,$$

where the subscripts *e/o* denote even/odd. In literature, a relation between even and odd cycles is known the Gnevyshevl - Ohl rule, which states that the strength of an even cycle is lower than the strength of the subsequent odd cycle.

We use the above relations to predict plage and sunspot area coverage during th SC-25 (see Fig. 2)

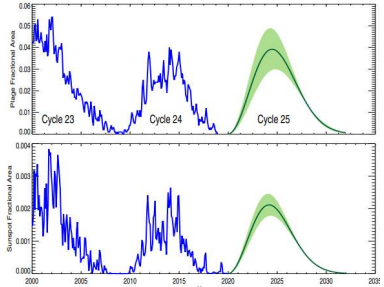

Fig. 2 *Prediction of plage coverage (top panel) and sunspot converage (bottom panel). The shadow green area defines the confidence limits.*

Long term component: decomposition of Φ

We decomposed the Solar Modulation Potential using the Empirical Mode Decomposition (EMD) algoritm. We considered the Intrinsic Mode Functions (IMFs) not present in sunspots coverage area and the monotonic residual signal (see Fig. 3). The long term (LT) modulation is computed as

(5) $$\Phi_{LT}(t) = \sum_{i=3}^{5} C_i \cdot IMF_i(t) + C_R \cdot R(t)$$

where the weights C_i and C_R are fixed using the Monte Carlo Markov Chain.

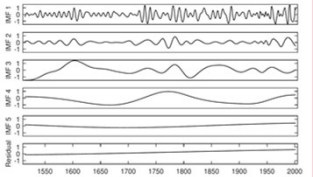

Fig. 3 *EMD of the standardized potential. IMF1 and IMF2 capture the shortest periods (11-22 yr). The residual shows the monotonic trend of the signal.*

TSI reconstruction

We reconstruct the solar irradiance *F* at time *t* as sum of different contributions from the j-.feature (quiet, network, facula and sunspot) weighted by respective coverage:

(6) $$F(t) = \sum_j \alpha_j(t) F_j.$$

We rewrite the Eq. (5), as a relative variation with respect to the radiative flux of the Quiet Sun and by adopting a linear correlation between network and facular coverage:

(7) $$\Delta F(t) = A_n \delta_n + \alpha_f(t)(B_n \delta_n + \delta_f) + \alpha_s(t)\delta_s = C_n + \alpha_f(t)\delta_{fn} + \alpha_s(t)\delta_s$$

The subscripts n,f and s indicate network, facular and sunspot components, respectively; C_n is a constant representing the product between the network contrast and the network coverage when $\alpha_f(t) = 0$; δ_{fn} is a linear combination of network and facular relative contrasts, and δ_s is the sunspot relative contrast. The values of C_n, δ_{fn} and δ_s are estimated by best fitting Eq.(6) with TSI measurements along 22th and 23th cycles. In order to reconstruct the TSI over temporal scales longer than the decadal one, we modulate the quiet network component C_n in the following way:

(8) $$\Delta F(t) = C_n mod_\Phi(t) + \alpha_f(t)\delta_{fn} + \alpha_s(t)\delta_s$$

The modulation function $mod_\Phi(t)$ is the long-term component of the Modulation Potential Φ_{LT} described in Eq. (5), properly normalized by best fitting the entire PMOD TSI composite. The final TSI reconstruction is shown in Fig. 4, compared with other models.

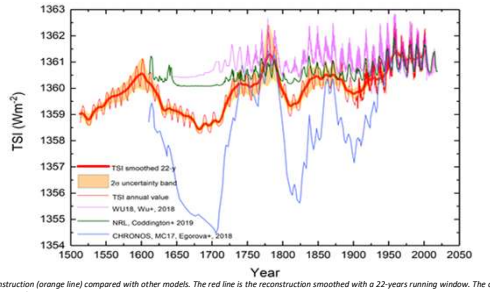

Fig. 4. *TSI reconstruction (orange line) compared with other models. The red line is the reconstruction smoothed with a 22-years running window. The orange area represents the 2-σ confidence level of the model.*

Forecast for 25th Cycle activity

Prediction of activity indices: MgII index and Radio Flux
Using an approach similar to sunspot and plage prediction we forecast two magnetic activity proxies: the core-to-wing ratio Mg II index and the Radio Flux F10.7. We apply the following parametric expressions:

(9) $$\frac{Mg\,II(t)}{Mg\,II_q} = \frac{\alpha_f(t)\delta^{(core)} + 1}{\alpha_f(t)\delta^{(wing)} + 1}, \qquad \frac{F^{(10.7)}(t)}{F_q^{(10.7)}} = [\alpha_f(t) + \alpha_s(t)]\delta^{(10.7)} + 1,$$

where $\delta^{(core)}$ and $\delta^{(wing)}$ are the relative facular contrasts of the intensity at the core and in the wings of MgII line, respectively, $\delta^{(10.7)}$ the radio contrast, while $MgII_q$ and $F_q^{(10.7)}$ are the values of index MgII and of F10.7 during a period of minimum. Unlike in the case of the Mg II index, for the F10.7 we take into account the contribution of both faculae and sunspots, but their contrast is modeled using a single parameter $\delta^{(10.7)}$ as both features contribute positively.

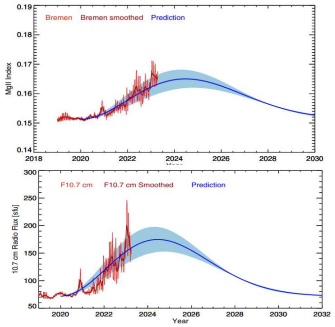

Fig. 5 Top Panel: *Prediction of the Mg II index for 25th Cycle and Bremen data composite.* Bottom Panel: *Prediction of the F10.7 for for 25th Cycle and CLS time series at 10.7 cm. In both plots, the solid line is the prediction smoothed using a gaussian kernel of one month bandwidth and the shaded area represents uncertainties in the predictions .*

Prediction of TSI : with a similar approach, using Eq. (7), we obtain the prediction for the TSI, that we compare with TSIS/TIM observations.

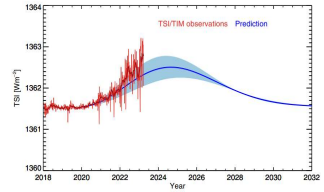

Fig. 6 *Prediction of the TSI for 25th Solar Cycle. The predicted irradiance values were increased by 1.07 W/m^2 to reconcile them with TSIS/TIM measurements.*